Influence of Bioconvection on the Electron Magnetohydrodynamic (EMHD) Fluid Flow

Abdullahi Gamsha Madaki[*], Rozaini Roslan[†], Abubakar Assidiq Hussaini[‡], Aminu Barde[§], Umar Aliyu Mujahid[**]

Abstract

In recent years, the important bioconvection phenomena with the use of nanoparticles has encountered basic industrial and technological applications. This study looked at how the bioconvection phenomenon affected the steady of EMHD nanofluid flow past an exponentially impermeable shrinking/stretching sheet. The system of partial differential equations is transformed into ordinary differential equations. We then employed similarity transformation in addition to non-dimensional quantities. Additionally, the shooting technique in Maple is used to numerically solve the resulting equations. We looked at how the model was affected by a few relevant parameters. The impact made by fluid over momentum, energy, concentration, along microorganism, including the Prandtl number, Peclet number, magnetic field, nanoparticle volume fraction parameter, electric conductivity, radiation parameter, bioconvection Lewis number, Weissenberg number, and more are shown graphically. By comparing the current results with the existing results in the literature, this technique is validated. Variations in some parameters yield the following result: momentum profile is a decreasing function when acted upon by nanoparticle volume fraction, magnetic field, impermeability parameter and variable viscosity parameter. Nonetheless radiation, electricity, variable viscosity decreases the temperature of the system. While temperature of the system is increased by Prandtl number, magnetic field and impermeability parameter. For larger values magnetic field, electricity causes concentration profile to falls down. Reverse is the case for radiation parameter and Prandtl number.

Keywords: Stretching/shrinking sheet, EMHD, Motile Microorganisms, Bioconvection, Bioconvection Lewis Number.

Introduction

In recent years, scientists have paid close attention to the nanomaterial because of its improved thermophysical properties. Their

[*]Department of Mathematics, Faculty of Sciences, Abubakar Tafawa Balewa University, Bauchi 740272, Nigeria, agmadaki@atbu.edu.ng

[†]Department of Mathematics and Statistics, Faculty of Applied Sciences and Technology, University Tun Hussein Onn Malaysia, Pagoh Campus, Muar 84600, Johor, Malaysia, rozaini@uthm.edu.my

[‡]Corresponding Author: Department of Mathematics Faculty of Sciences, Abubakar Tafawa Balewa University, Bauchi 740272, Nigeria, ahabubakar.pg@atbu.edu.ng

[§]Department of Mathematics Faculty of Sciences, Abubakar Tafawa Balewa University, Bauchi 740272, Nigeria, bardealamin@yahoo.com

[**]Department of Mathematics, Faculty of Sciences, Abubakar Tafawa Balewa University, Bauchi 740272, Nigeria, umaraliyumujahid@gmail.com

prospective uses in chemical engineering, solar energy systems, microelectronics, biomedical applications, material processing industries, energy consumption, etc., are what give these nanomaterials their intriguing significance. Choi (1995) conducted a groundbreaking study on nanoparticles, demonstrating that their interaction with different base liquids might enhance the thermophysical properties of conventional base liquids. This unique concept prompts the scientific community to use a variety of fluid models in a range of combinations to explain the characteristics of nanoparticles. For example, Malik et al. (2016) investigated the viscous dissipation effect with MHD.

Using a porous media, Manjunatha et al. (2017) examined the radiation effect when a heat source was present. When solid nanoparticles come into contact with base fluids, nanofluid is created Common base fluids include water, oil, and so forth. Because of their special chemical and physical characteristics, nanofluids have a wide range of industrial uses. Nanofluids are used in a wide range of engineering applications, including fuel cells, microelectronics, coolants, and home freezers. Additionally, Khan & Pop (2010), Madaki et al. (2024).

Khan et al. (2024) examined the impacts of bioconvection using nanofluid as a primary biofuel application. In order to assess the effects of heat radiation and activation energy. The Cattaneo-Christov double diffusion theory is also seen. In the latest technologies, nanofluids react quickly to a range of demands. This study included applications in the fields of contemporary nanotechnology, microelectronics, nano-biopolymers, biomedicine, and biotechnology as well as in the treatment of cancer treatments, fuel cell technology, and power generating and atomic reactor cooling. The partial differential equations that constitute the basis of their study are gradually reduced to a set of highly nonlinear mathematical representations of ordinary differential equations by applying the proper similarity transformation. The MATLAB software's bvp4c tool and a well-known shooting strategy are then used to numerically approach these forms. The key aim of the analysis by Nabwey et al. (2022) was to scrutinize the trend of swimming motile microorganisms in a time-dependent MHD 2-D convectional flow of Carreau-nanomaterials around an oblique cylinder. The flow problem was considered using the new concepts of fluctuating magnetic field and non-uniform thermal conductivity. Absolute drag force was found to decrease with rising Weissenberg number along mixed convection factor and to increase accompanied by rising curvature, unsteadiness, magnetic field, and power-law factors. The primary objective of research conducted by Francis et al. (2024) was to investigate the flow properties of a bio-convective nanofluid that exhibited non-Newtonian behavioral patterns.

They specifically used the Eyring-Powell fluid framework in their study. The flow was investigated in relation to an upright cone. They also considered the impacts of Brownian motion, thermophoresis, magnetohydrodynamics (MHD), and heat radiation. Gaining a deeper comprehension of the mechanics related to mass and heat transport was the aim of their research. They examined several physical facets associated with data analysis in order to fully comprehend the model. The main objective of the study by Priyadharshini et al. (2023) was to investigate how thermophoresis diffusion and Brownian motion interactions. Additionally, as a successful implementation of this study's uniqueness, the physical quantities pertaining to the non-dimensional parameters are predicted by using Multiple Linear Regression (MLR) in Machine Learning (ML). For upcoming researchers, these cutting-edge methods can aid in advancing technology and development. Their discovery has practical implications for cancer preventative therapy, microbial motility in mixed fluids, and bio-remediation. Other related researches in the same vein includes (Bilal et al., 2024; Imran et al., 2024; Zhang et al., 2022; Awwad et al., 2023; Ahmed et al., 2022).

Recent developments in fluid dynamics have highlighted the growing importance of magnetohydrodynamic (MHD) nanofluid flows, particularly in the presence of bioconvection, thermal radiation, and chemical reactions. Abdelmalek et al. (2021) formulated a mathematical model for Williamson nanofluid flow over a stretching cylinder incorporating variable thermal conductivity, activation energy, and higher-order slip effects, while Bhatti et al. (2018) analyzed MHD nanofluid flow with gyrotactic microorganisms under thermal radiation and chemical reaction influences. The pioneering work of Kuznetsov (2010) established the onset of nanofluid bioconvection in suspensions containing nanoparticles and motile microorganisms, which was further extended by Mutuku and Makinde (2014) to hydromagnetic bioconvection over a permeable vertical surface. In addition, Vinita & Poply (2020) investigated MHD slip flow and heat transfer of nanofluids past a stretching cylinder, emphasizing the role of external velocity conditions. More recently, Hussaini et al. (2022) explored convective MHD nanofluid flow over an impermeable stretching surface using a numerical approach, whereas Gamsha et al. (2022) examined the combined effects of chemical reaction, heat generation, and absorption on MHD stagnation point flow with solar radiation. Collectively, these studies provide a comprehensive foundation for understanding the complex interplay of physical mechanisms governing nanofluid flow and heat transfer in modern applied mathematics and engineering systems.

Mathematical Modeling

By using a small magnetic Reynolds number, we were able to create both an electric and magnetic field. They are continuously used at their highest level of intensity. It is believed that viscous dissipation has a significant role. It is believed that the stretching/shrinking sheet's surface temperature varies, as illustrated in Figure 1 below. The equations governing the movement for the Boussinesq approximation are as in Shehzad et al. (2023), assuming the boundary layer approximation is correct.

$$\frac{\partial u}{\partial x}+\frac{\partial v}{\partial y}=0, \tag{1}$$

$$u\frac{\partial u}{\partial x}+v\frac{\partial v}{\partial y}=\frac{1}{\rho_{nf}}\Big[\mu_{nf}\frac{\partial^2 u}{\partial y^2}-\sigma_{nf}(E(x)B(x)-B(x)^2u)+ g(\rho\beta)_{nf}(T-T_\infty)\Big]+\frac{\mu_e}{k}\frac{1}{\rho_{nf}}\big[(1-C_\infty)_{\rho f}\beta^* g(T-T_\infty)-\big(\rho_p-\rho_f\big)g(C-C_\infty)-(n-n_\infty)g\gamma^*\big(\rho_m-\rho_f\big)\big]=0, \tag{2}$$

$$(\rho Cp)_{nf}\left(u\frac{\partial T}{\partial x}+v\frac{\partial T}{\partial y}\right)=\left(k_{nf}+\frac{16T_\infty^3\sigma}{3k_fk_f^*}\right)\frac{\partial^2 T}{\partial y^2}+\sigma_{nf}(uB(x)-E(x))^2+ \frac{Q}{\rho_{nf}}(T-T_\infty)=0, \tag{3}$$

$$u\frac{\partial C}{\partial x}+v\frac{\partial C}{\partial y}=D_B\frac{\partial^2 C}{\partial y^2}+\frac{D_T}{T_\infty}\left(\frac{\partial^2 T}{\partial y^2}\right)-K(C-C_\infty), \tag{4}$$

$$u\frac{\partial N}{\partial x}+v\frac{\partial N}{\partial y}=D_m\left(\frac{\partial^2 N}{\partial x^2}\right)-\frac{b^*W_c}{(C_w-C_\infty)}\left[\frac{\partial}{\partial x}\left(N\frac{\partial C}{\partial x}\right)\right], \tag{5}$$

With boundary conditions:

$$u=ax, v=v_w(x)=0, -k\frac{\partial T}{dy}=h\big(T_f-T\big), C=C_w(x)aty=0,$$

$$u=0, T=T_\infty, C=C_\infty asy\to\infty \tag{6}$$

Assuming the surface temperature fluctuates in the way outlined below:

$$T_w(x)-T_\infty=Ax^n, \tag{7}$$

The Momentum $f(\eta)$ and Temperature $\theta(\eta)$ the similarity term is given by ηwhile ψ is the stream term

$$\eta=y\sqrt{\frac{a}{v}}, u=\frac{\partial\psi}{\partial y}, v=-\frac{\partial\psi}{\partial x}, \psi=xf'(\eta)\sqrt{av}, \theta(\eta)=\frac{T-T_\infty}{T_w-T_\infty}\Rightarrow T=\theta T_w,$$

$$\phi(\eta)=\frac{C-C_\infty}{C_w-C_\infty}\Rightarrow C=\phi C_w, \chi=\frac{N-N_\infty}{N_w-N_\infty}\Rightarrow N=\chi N_w \tag{8}$$

$$u=\frac{\partial\psi}{\partial y}=Uf'andv=-\frac{\partial\psi}{\partial x}=\frac{1}{2}\sqrt{\frac{uv}{x}}\big(\eta f'-f\big) \tag{9}$$

Notably, prime indicates differentiation regardingη. The outcome of applying Eqs. (6) to (8) to reduce Equation (1) to Equation (5) is as follows.

$$f''' + (1-\phi)^{2.5}\left\{\begin{array}{l}(1-\phi)+\phi\left(\frac{\rho_s}{\rho_f}\right)(-2f'^2+f''f)\\ -2\left(\begin{array}{c}1+\frac{3\phi\left(\frac{\sigma_s}{\sigma_f}-1\right)}{\left(\frac{\sigma_s}{\sigma_f}+2\right)-\left(\frac{\sigma_s}{\sigma_f}-1\right)\phi}\sigma_f\\ +\xi\left((1-\phi)+\phi\left(\frac{\rho_s}{\rho_f}\right)\right)\end{array}\right)\end{array}\right\} = 0, \quad (10)$$

$$\left(\frac{k_{nf}}{k_f}+\frac{4}{3}Rd\right)\theta'' + Pr\left\{(1-\phi)+\phi\frac{(\rho Cp)_s}{(\rho Cp)_f}\left(f\theta' - 4f'\theta\right)\right\} + A_2 EcM\left(f' - E_1\right)^2 + \lambda\theta = 0, \quad (11)$$

$$\varphi'' + Lef\varphi' - 2Lef'\varphi' + \frac{Nt}{Nb}\theta'' - \gamma\varphi = 0, \quad (12)$$

$$(1-\phi)\chi'' + Lb(1-\phi)f'\chi - Pe\left(\varphi''(\chi+\Omega_1)\right) + \chi'\varphi' = 0, \quad (13)$$

The subsequent boundary conditions are applicable:

$$f'(0) = \lambda_2, f(0) = S, \theta(0) = \delta\left[1-\theta'(0)\right], \varphi(0) = 1, \chi(0) = 1$$
$$f'(\infty) = 0, \theta(\infty) = 0, \varphi(\infty) = 0, \chi(\infty) = 0, \quad (14)$$

Numerical Results

The system of differential Equations (10) – (13) used in this investigation using the shooting technique in the Maple software, Equation (14) is numerically solved along the boundary conditions. Finding the effects of different fluid parameters, such as the magnetic parameter M, the thermal radiation parameter Rd, the bioconvection Lewis number parameter Lb, the nanoparticle volume fraction parameter, the Peclet number parameter Pe, and other relevant parameters on velocity, temperature field, nanoparticle concentration, and gyrotactic microorganism profiles, is the primary goal of solving these equations. Tables and graphs are used to display the results (The thermo-physical properties of the working fluid are provided in Table 1, while the governing dimensionless parameters are listed in Table 2. Additionally, the properties of the base fluid and nanoparticles are summarized in Table 3. To ensure the accuracy of the present results, a comparison with existing literature is carried out, and the results are presented in Table 4, showing excellent agreement). Using a range of values instead of precise numbers for the parameters may yield better outcomes in real-world implementations of the research. The graphical behavior of the system is illustrated in Figures 1–10, where Figure 1 shows the effect of nanoparticle volume fraction on the momentum profile, Figure 2 depicts its influence on nanoparticle concentration, Figures 3 and 4 present the effects of thermal radiation and Prandtl number on the motile microorganism profile, respectively, Figure 5

illustrates the variation with Peclet number, Figures 6 and 7 demonstrate the influence of magnetic parameter on momentum and temperature profiles, respectively, Figure 8 shows the effect of impermeability parameter on momentum, while Figures 9 and 10 display the effects of variable viscosity and electrical parameter on temperature and concentration profiles, respectively.

Table 1: Thermo-physical aspects of the nanofluid as used by Shehzad et al. (2023).

Hybrid nanofluid	*Properties*
$\sigma_{nf} = 1 + \frac{3\phi\left(\frac{\sigma_s}{\sigma_f}-1\right)}{\left(\frac{\sigma_s}{\sigma_f}+2\right)-\left(\frac{\sigma_s}{\sigma_f}-1\right)}\sigma_f$	Electrical Conductivity (k)
$\rho_{nf} = (1-\phi)_{\rho f} + \phi_{\rho s}$	Density (ρ)
$\alpha_{nf} = \frac{k_{nf}}{(\rho Cp)_{nf}}$	Thermal Conductivity (k)
$\frac{\mu_{hnf}}{\mu_f} = \frac{1}{(1-\varphi_{hnf})^{2.5}}$	Dynamic Viscosity (μ)
$(\rho C_p)_{hnf} = (1-\varphi_{hnf})(\rho C_p)_f + \varphi_1(\rho C_p)_{s1} + \varphi_2(\rho C_p)_{s2}$	Heat Capacity $\left(\rho C_p\right)$
$(\rho\beta)_{nf}$	Thermal expansion

Table 2: Parameters involved in the ODEs as used by Shehzad et al. (2023).

Graham's number $Gr = \frac{L^3 g\beta_f T_0}{\vartheta f^2}$	Mixed convection parameter $\Lambda = \frac{\beta^*(1-C_\infty)(T_w-T_\infty)}{U_0^2}$
Thermophoresis $Nt = \frac{(\rho C)_p D_T(T_f-T_\infty)}{(\rho C)_f T_\infty v}$	Prandtl number $Pr = \frac{\vartheta(\rho Cp)_f}{k_f}$
Buoyancy ratio parameter $Nr = \frac{(\rho_p-\rho_f)(C_w-C_\infty)}{(1-C_\infty)U_0^2(T_w-T_\infty)\beta^*}$	Bioconvection Rayleigh number $Nc = \frac{\gamma(\rho_m-\rho_f)(N_w-N_\infty)}{(1-C_\infty)U_0^2(T_w-T_\infty)\beta^*}$
Brownian motion parameter $Nb = \frac{(\rho C)_p D_B(C_w-C_\infty)}{(\rho C)_f v}$	Curvature parameter $\gamma = \frac{hf}{k}\sqrt{\frac{vl}{U_0}}$
Peclet number $Pe = \frac{b^* W_c}{D_m}$	Heat generation parameter. $\lambda = \frac{\vartheta Q}{U_w T_w \rho_{nf}}$
Radiation parameter $Rd = \frac{4T_\infty^3\sigma^*}{k_f k_f^*}$	Bioconvection Lewis number $Lb = \frac{v}{D_m}$
Thermal slip parameter $\delta = B\sqrt{\frac{U_w}{2\vartheta L}}$	Schmidt number $Sc = \frac{v}{D_B}$
Electric Field Parameter $E_1 = \frac{2LE_0}{\sigma B_0^2 U_w}$	Magnetic parameter $M = \frac{\sigma B_0^2 L}{\rho U_w}$
Variable Viscosity $A_2 = 2\vartheta U_w(T_w - T_\infty)$	Impermeability Parameter $k_1 = \frac{2LU_w\mu_e}{k}$
Eckert number $Ec = \frac{U_w^2}{\vartheta(T_w(x)-T_\infty)}$	Suction/ Injection Parameter $S = -\sqrt{\frac{2L}{\vartheta U_w}}$
Stretching/ Shrinking parameter $\lambda_1 = A\sqrt{\frac{\vartheta U_w}{2L}}$	Weissenberg number $\Omega_1 = \frac{N_\infty}{N_w-N_\infty}$

Table 3: Thermo-physical features of nanoparticles and base liquid (water) as used by Shehzad et al. (2023).

water(Fe_3O_4)	Base fluid	Nanoparticle
$C_p\left(\frac{J}{kg}.K^{-1}\right)$	4179	670
$\rho\left(\frac{kg}{m^3}\right)$	997.1	5180
$k\left(\frac{W}{m}.K^{-1}\right)$	0.61	3080.4
$\beta \times 10^{-5}(k^{-1})$	21	20.6

Table 4: Comparative values of $f''(0)$ and $-\theta'(0)$ with published results of Shehzad et al. (2023).

Varying parameter	Shehzad et al. (2023)		Present result	
S	$f''(0)$	$-\theta'(0)$	$f''(0)$	$-\theta'(0)$
0	1.28181	0.767768	1.28181	0.767766
0.3	-	-	1.38501	0.896891
0.6	1.5982	1.014571	1.59828	1.014580
0.8	-	-	1.70173	1.732067
1.0	-	-	1.98016	2.497629

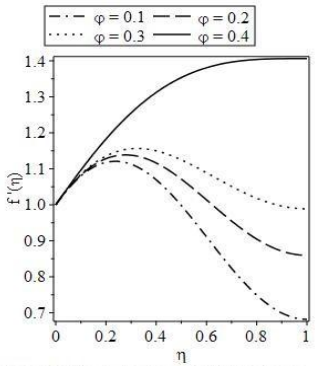

Figure 1: Influence of nanoparticle volume fraction parameter on momentum profile.

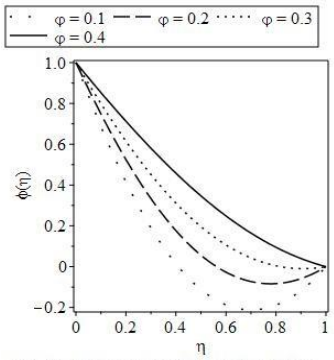

Figure 2: Influence of nanoparticle volume fraction on nanoparticle concentration profile.

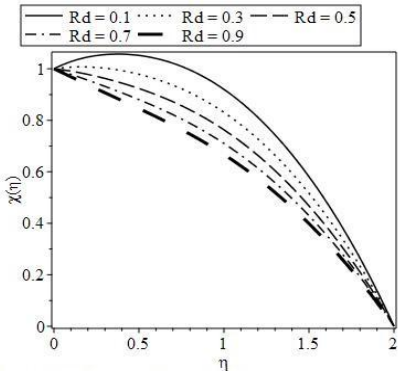

Figure 3: influence of thermophoresis parameter on motile microorganism profile.

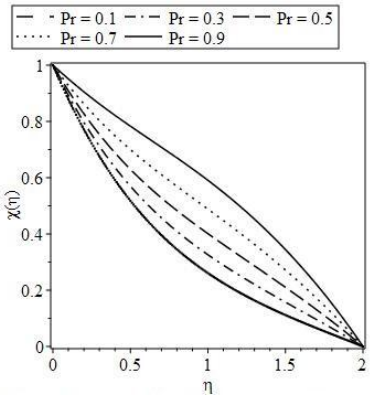

Figure 4: influence of thermophoresis parameter on motile microorganism profile.

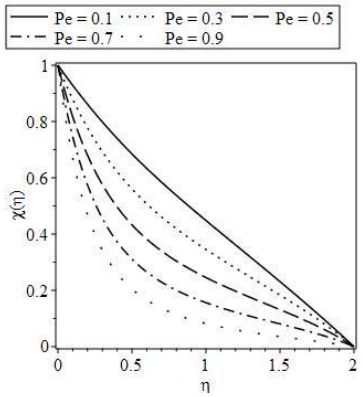

Figure 5: influence of Peclet number parameter on motile microorganism profile.

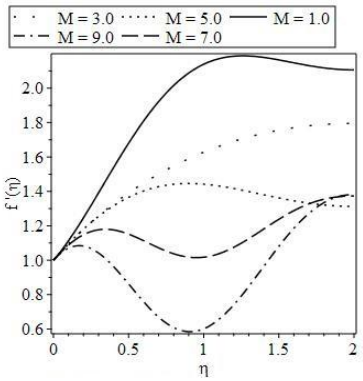

Figure 6: influence of Magnetic parameter on momentum profile

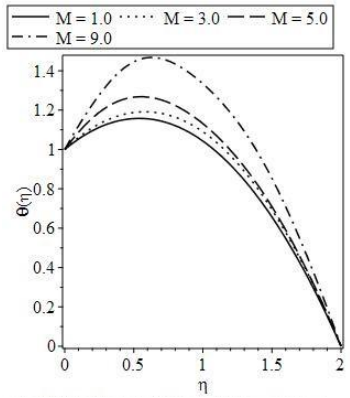

Figure 7: influence of Magnetic parameter on temperature profile.

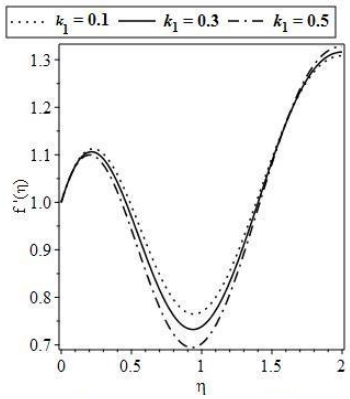

Figure 8: influence of impermeability parameter on momentum profile.

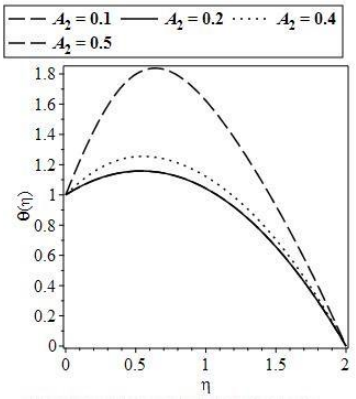

Figure 9: influence of variable viscosity parameter on temperature profile.

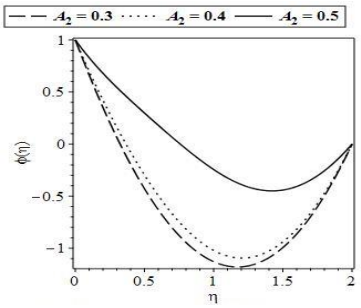

Figure 10: influence of variable viscosity parameter on concentration profile.

Discussion

Figure 1 is plotted to display the influence of nanoparticle volume fraction parameter over the profile of momentum. As the parameter increases the momentum profile decline. Clearly observing Figure 2, revealed that increase in the values of nanoparticle volume fraction parameter (ϕ) decreases the nanoparticle concentration profile. The impact of thermal parameter (Rd) over the motile microorganism profile is exhibited in Figure 3. From this figure, it reveals in thermal radiation parameter plunges the temperature of the system; Rd is constantly inspired by the surrounding temperature. Consequently, the fluid temperature is condensed due to a solid effect of Rd. Furthermore, the temperature ratio parameters beyond valuations classify increasing wall temperature in relation to the fluid's ambient temperature. After that, the liquid's temperature will drop. Significantly, the radiation process is characterized by a radiation dimensionless parameter that decreases the temperature by adding heat to the fluid. Is obviously intended to illustrate how thermal radiation affects the microorganism profile; in this instance, it is evident that with every rise in the parameter values, the microorganism profile of

the system decreases. Figure 4 display the impacts of Prandtl number parameter (Pr) over the microorganism profile. A decrease in heat diffusion is correlated with an improvement in Pr. Additionally, a convective flow is created as a result of thermophoresis, which causes the hot liquid particles to move from a hot to a cold region, in this way, the microorganism profile decreases with each increase in the parameter values.

Figure 5 is drawn to examine the microorganism profiles via greater Peclet number parameter Pe. Peclet number and microbe diffusivity are physically connected. Higher Pe values cause the diffusivity of microorganisms to decrease, which lowers the microbial profile. This proves that Pe has no effect on the rate at which mass and heat are transmitted. Figure 6 illustrates how the momentum boundary layer thins at the plate as the magnetic parameter increases. Variations in the magnetic parameters lead to an increase in electrical movements, which in turn causes an increase in Lorentz force, which causes the momentum profile to decrease. Also, description on the influence of M on temperature is achieved in Figure 7. Here, it is observed that the temperature profile is enhanced with the enhancement in magnetic field parameter (M).

Figure 8 displays the momentum profile for a range of impermeability parameter (k1) values. We discovered that when the parameter increases, the momentum drops. As a result, the boundary layer becomes thinner. This occurs as a result of the Lorentz force, which is created when magnetic and electric fields interact when the electrically conductive fluid is moving. The resulting Lorentz force improves the fluid motion in the boundary layer region, reducing the thickness of the momentum.

However, the heat transfer rate close to the plate slightly improves as the parameter increases. The growing temperature differential between the plate and the surrounding air is the cause of this. Figs. 10 is on the variation of temperature profile over the variable viscosity parameter (E1). It can be observed that on Figure 9 shows how an electricity parameter (E1) affects the temperature profile. The temperature profile somewhat decreases and the boundary layer gets thinner as the parameter increases. This is the case because a lower variable viscosity value means that less heat may pass the fluid.

The impact of the electrical parameter (E1) on the concentration profile is seen on Figure 10. The figures show that the mass boundary layer gains from a drop in fluid concentration when the parameter is increased. The reaction rate is influenced by the species concentration. Heterogeneous interactions between two different states of matter produce new chemicals when fluid particles come into touch with the atmosphere.

This figure highlights the buoyancy effect caused by concentration gradients, demonstrating the safety of the chemical process.

Conclusions

In this study, we exploited the influence of bioconvection phenomenon in the flow of steady EMHD nanofluid past on an exponential impermeable shrinking/stretching sheet. The results of this study include the effects of EMHD, the volume fraction parameter of nanoparticles, thermal radiation, and the Bioconvection Lewis number, magnetic field, mixed convection parameter, Prandtl number, and Weissenberg number, among other factors, on the flow and heat transport of nanofluid in terms of momentum, temperature, concentration distribution, and microorganism profiles. The following are the current problem's final results:

- Radiation parameter, Prandtl number, Peclet number, Weissemberg number as well as bioconvection Lewis number shows no effect on the momentum profile.
- However, mixed convection parameter as well as electricity causes the momentum to fluctuate.
- Momentum profile is a decreasing function when acted upon by nanoparticle volume fraction, magnetic field, impermeability parameter and variable viscosity parameter.
- On the other hand, Peclet number, Weissenberg and bioconvection Lewis number shows no effect on the temperature profile.
- However, radiation, electricity and variable viscosity parameter decreases the temperature of the system.
- Temperature of the system is increased by Prandtl number, magnetic field and impermeability parameter.
- For larger values magnetic field with electricity causes concentration profile to falls down. Reverse is the case for radiation parameter and Prandtl number.
- Impermeability parameter is the only parameter which has no effect on microorganism profile.
- The profile of microorganisms varies less for radiation, Prandtl number, Peclet number, mixed convection parameter. For Bioconvection Lewis number, the opposite is true.

Conflict of Interest: Author (s) declare that they do not have any conflict of interest.

References

Abdelmalek, Z., Khan, S. U., Waqas, H., Riaz, A., Khan, I. A., & Tlili, I. (2021). A mathematical model for bioconvection flow of Williamson nanofluid over a stretching cylinder featuring variable thermal conductivity, activation energy and second-order slip. *Journal of Thermal Analysis and Calorimetry, 144*(1), 205-217.

Ahmed, M. F., Zaib, A., Ali, F., Bafakeeh, O. T., Tag-ElDin, E. S. M., Guedri, K., ... & Khan, M. I. (2022). Numerical computation for gyrotactic microorganisms in MHD radiative Eyring–Powell nanomaterial flow by a static/moving wedge with Darcy–Forchheimer relation. *Micromachines*, *13*(10), 1768.

Awwad, F. A., Ismail, E. A. A., Khan, W., Gul, T., & Khan, A. S. (2023). Comparative numerical analysis for the error estimation of fluid flow over an inclined axisymmetric cylinder with a gyrotactic microbe. *Symmetry*, *15*(9), 1811 1825.

Bhatti, M. M., Mishra, S. R., Abbas, T., & Rashidi, M. M. (2018). A mathematical model of MHD nanofluid flow having gyrotactic microorganisms with thermal radiation and chemical reaction effects. *Neural Computing and Applications*, *30*(4), 1237–1249.

Bilal, S., Asadullah, & Malik, M. Y. (2024). Computational analysis to explore bioconvective Williamson nanofluid non-Darcianflow over a convective cylindrical surface with gyrotactic microorganisms and activation energy aspects. *BioNanoScience*, *14*(3), 725–747.

Choi, S. U. (1995, November). Enhancing thermal conductivity of fluids with nanoparticles. In *ASME international mechanical engineering congress and exposition* (Vol. 17421, pp. 99-105). American Society of Mechanical Engineers.

Francis, P., Sambath, P., & Chamkha, A. J. (2024). Dual diffusion effects on radiated bio-convective magnetohydrodynamics Powell–Eyring nanofluid flow along a vertical cone surface. *Scientia Iranica, 31*(1).

Hussaini, A. A., Gamsha, A. M., Alaramma, S. K., Barde, A., & Abdullahi, I. (2022). Numerical approach for convective magnetohydrodynamic (MHD) nanofluid flow with impermeable stretching surface. *The Sciencetech*, *3*(1).

Gamsha, A. M., Hussaini, A. A., Musa, A. M., & Alaramma, S. K. (2022). Simultaneous Effects of Chemical Reaction, Heat Generation, Absorption on Solar Radiation over Magneto Hydrodynamics Stagnation Point Flow and Heat Transfer of a Nanofluid Over a Stretching Sheet. *The Sciencetech*, *3*(4).

Imran, M., Basit, M. A., Yasmin, S., Khan, S. A., Elagan, S. K., Akgül, A., & Hassan, A. M. (2024). Numerical study of a mathematical model of bioconvective Maxwell nanofluid flow through a porous stretching surface with Nield/convective boundary constraints. *Scientific Reports*, 14(1), 1873.

Khan, S. A., Ramzan, A., Ali, M., Imran, M., Machado, J. M., Kedzia, K., & Jan, A. Z. (2024). Numerical simulation of bioconvection Maxwell nanofluid flow due to stretching/shrinking cylinder with gyrotactic motile microorganisms: a biofuel applications. *BioNanoScience*, *14*(5), 4895-4909.

Khan, W. A., & Pop, I. (2010). Boundary-layer flow of a nanofluid past a stretching sheet. *International journal of heat and mass transfer*, *53*(11-12), 2477-2483.

Kuznetsov, A. V. (2010). The onset of nanofluid bioconvection in a suspension containing both nanoparticles and gyrotactic microorganisms. *International Communications in Heat and Mass Transfer*, 37(10), 1421–1425.

Madaki, A. G., Hussaini, A. A., Roslan, R., & Umar, A. B. (2024). Numerical simulation for an electron magnetohydrodynamic nanofluid with iron oxide (Fe_3O_4) under the triple effects of electric field, heat generation/absorption, and impermeability of the surface. *International Journal of Scientific Research in Mathematical and Statistical Sciences*, *11*(5), 11–22.

Malik, M. Y., Hussain, A., Salahuddin, T., & Awais, M. (2016). Effects of viscous dissipation on MHD boundary layer flow of Sisko fluid over a stretching cylinder. *AIP Advances*, *6*(3).

Manjunatha, P. T., Gireesha, B. J., & Prasannakumara, B. C. (2017). Effect of radiation on flow and heat transfer of MHD dusty fluid over a stretching cylinder embedded in a porous medium in presence of heat source. *International Journal of Applied and Computational Mathematics*, *3*(1), 293-310.

Mutuku, W. N., & Makinde, O. D. (2014). Hydromagnetic bioconvection of nanofluid over a permeable vertical plate due to gyrotactic microorganisms. *Computers & Fluids*, *95*, 88-97.

Nabwey, H. A., Alshber, S. I., Rashad, A. M., & Mahdy, A. E. N. (2022). Influence of bioconvection and chemical reaction on magneto—Carreau nanofluid flow through an inclined cylinder. *Mathematics*, *10*(3), 504.

Priyadharshini, P., Karpagam, V., Shah, N. A., & Alshehri, M. H. (2023). Bio-convection effects of MHD Williamson fluid flow over a symmetrically stretching sheet: Machine learning. *Symmetry*, *15*(9), 1684–1702.

Shehzad, S. A., Shaikh, A. A., Shah, S. F., Lanjwani, H. B., Anwar, M. I., & Kumar, S. (2023). Numerical investigation of magnetized thermally radiative Fe_3O_4–water base nanofluid. *Chemical Physics Letters, 824(1)*, 140571.

Vinita, V., & Poply, V. (2020). Impact of outer velocity MHD slip flow and heat transfer of nanofluid past a stretching cylinder. *Materials Today: Proceedings*, *26*, 3429-3435.

Zhang, X., Yang, D., Rehman, M. I. U., Mousa, A. A., & Hamid, A. (2022). Numerical simulation of bioconvection radiative flow of Williamson nanofluid past a vertical stretching cylinder with activation energy and swimming microorganisms. *Case Studies in Thermal Engineering*, *33*, 101977.